

# 1 **Complex nanostructures in diamond**

2  
3 **Meteoritic diamonds formed during bolide impacts on Earth and diamond-related materials**  
4 **synthesized by compressing graphite contain a wide variety of complex nanostructures. This**  
5 **Comment highlights and classifies this structural complexity by a systematic hierarchical**  
6 **approach, and discusses the perspectives on nanostructure and properties engineering of**  
7 **diamond-related materials.**

8  
9 Péter Németh, Kit McColl, Laurence A.J. Garvie, Christoph G. Salzmann, Mara Murri and Paul F.  
10 McMillan

11  
12 Elemental carbon continues to surprise by its versatility in bonding resulting in a multitude of  
13 structures with markedly different material properties. Graphite and diamond, which are minerals  
14 known since antiquity, have been applied and further developed in various applications according to  
15 their distinct properties determined by the nature of their interatomic linkages. Graphite is a  
16 semimetallic  $sp^2$ -bonded layered solid that is widely used as a lubricant and highly absorbent  
17 material associated with its weak interlayer bonding. It is the most stable carbon phase at ambient  
18 conditions. Varieties of graphitic carbon reversibly intercalate ions and can therefore be used as  
19 anodes in energy storage devices. In contrast, diamond is a superhard wide bandgap insulator. It is  
20 transparent throughout most of the electromagnetic spectrum and possesses remarkably high  
21 thermal conductivity. These properties are the result of its tetrahedrally connected  $sp^3$ -bonded  
22 network of carbon atoms<sup>1</sup>. First prized as a rare gem mineral with near-mythical properties, its  
23 name is derived from the Greek ἀδάμας (the indomitable one) reflecting its extreme resistance to  
24 mechanical, heat and chemical stress. Its qualities have been harnessed for cutting and grinding  
25 applications. Synthetic diamond production is a multi-billion \$/yr worldwide industry estimated at  
26 near 4.41 billion carats per year<sup>2</sup>. Nanosized diamonds formed by explosive shock processes are  
27 commercially available, whereas highly crystalline diamond films used as protective coatings and in  
28 optoelectronic devices are grown by vapour deposition techniques. There is the tantalizing  
29 possibility of the existence of other carbon forms with properties that rival those of diamond; search  
30 for these materials is under way in laboratories around the world<sup>3,4</sup>. Recent investigations have  
31 expanded the list of elemental carbon varieties to include fullerenes, nanotubes, single- to few-  
32 layered graphene and new crystalline materials. The menagerie of polymorphic carbon structure  
33 types continues to grow as new examples become identified among samples formed naturally  
34 within meteorites and by bolide impacts on Earth, produced in the laboratory, or are predicted by  
35 theoretical calculations<sup>5-9</sup>.

36  
37 The structures of natural and synthetic carbon materials are typically characterized using X-ray  
38 diffraction (XRD) and optical spectroscopic techniques, particularly Raman spectroscopy<sup>10-11</sup>. The  
39 nanoscale features present within these materials are increasingly being studied using high-  
40 resolution transmission electron microscopy (HRTEM) imaging and diffraction techniques<sup>12-16</sup>.  
41 Aberration-corrected HRTEM studies are now revealing unprecedented structural detail and  
42 complexity within diamonds and related materials that are recovered from meteorites and impactites  
43 as well as laboratory-shocked samples<sup>12, 14, 15</sup>. The results are leading to the discovery of new  
44 structural motifs and re-interpretation of previously reported polymorphic forms (Fig. 1). The newly  
45 identified features include multiple intergrowths and domains of nanotwinned stacking within  $sp^3$ -  
46 bonded diamond<sup>10-12,15</sup>, regions with  $sp^3$ - and  $sp^2$ -structured units coherently bonded to each other  
47<sup>13,14</sup>, concentric nanodiamond-containing carbon cages<sup>16</sup>, and nanoscale patterns with unusual  
48 symmetry within the dense carbon matrix<sup>15</sup>. It is a challenge to unravel the complexity of these  
49 nanostructures that are often observed within the same sample and to determine both the  
50 relationships between them and how they might arise as a function of the original synthesis and  
51 subsequent processing conditions. This Comment aims to present a hierarchical description of these  
52 different nanostructured motifs within a range of natural and laboratory-shocked samples and show

53 how they might be related within a structural map of  $sp^3$ - to  $sp^2$ -bonded polymorphs sorted as a  
54 function of their energy-volume relationships. In addition, we examine how the presence of these  
55 varied and complex nanostructures could give rise to potentially useful mechanical, thermal and  
56 optoelectronic properties and how these might be engineered to produce new families of next-  
57 generation diamond-related materials<sup>14,17,18</sup>.

58

### 59 **Cubic and hexagonal diamond**

60 Diamond contains tetrahedrally bonded carbon atoms that are covalently linked to form six-  
61 membered rings in a "chair" conformation as found in the cyclohexane molecule. The diamond  
62 structure is usefully described based on corrugated layers formed from these rings. We refer to  
63 these layers as fully saturated "diaphane" units, by extension from the term "graphene" used to  
64 describe a single plane of  $sp^2$ -bonded carbon atoms<sup>6</sup>. In diamond, identically oriented diaphane  
65 layers stack normal to the cubic (111) axis, accompanied by a shift half-way across the diagonal of  
66 the six-membered rings. This stacking leads to a cubic (*c*) packing arrangement of the carbon atoms  
67 for the cubic diamond polytype.

68

69 A metastable  $sp^3$ -bonded carbon structure, first identified from high-pressure high-temperature  
70 (HPHT) laboratory syntheses and also found within natural impact-formed diamonds, displays  
71 hexagonal (*h*) features in its XRD pattern<sup>19,20</sup>. These diffraction features were associated with an  
72 ordered polytype structure in which the stacking pattern includes an orientation reversal between  
73 successive  $sp^3$ -bonded "diaphane" layers resulting in a 50:50 mix of "chair" and "boat"  
74 configurations of the cyclohexane rings. Both this structure type and the new mineral were named  
75 "lonsdaleite" to honour the crystallographic contributions of Dame Kathleen Lonsdale<sup>21</sup>.  
76 Identification of such hexagonal features in the XRD patterns and corresponding Raman spectra of  
77 diamonds recovered from meteorites and bolide impact sites has become established as an  
78 important mineralogical marker for the shock conditions experienced during impact events.

79

80 Both natural and laboratory-shocked samples are typically described in terms of "pure" cubic  
81 diamond and lonsdaleite polytype structures, sometimes accompanied by graphite, that are  
82 interpreted as nanoscale mixtures of the proposed end-members. Laboratory experiments carried  
83 out to reproduce and extend the P-T conditions of natural shock events have adopted a similar level  
84 of interpretation<sup>22,23</sup>. However, this view of describing the complex nanostructures present within  
85 natural impact and laboratory-produced diamonds as mixtures of these two polytype structures is  
86 now shown to be incorrect.

87

### 88 **Cubic-hexagonal stacking disorder and nanotwinned structures within diamond**

89 It was first noted that the hexagonal diffraction features assigned to "lonsdaleite" arise from non-  
90 repetitive structures and should instead be interpreted with normal cubic diamond containing a high  
91 density of stacking faults and nanoscale twins (Fig. 1)<sup>12</sup>. This interpretation was based on detailed  
92 HRTEM studies of samples from the Canyon Diablo meteorite, the type material from which the  
93 mineral lonsdaleite was first described<sup>19,20</sup>. A range of *h-c* stacked sequences is well known to  
94 occur among SiC, BN and other  $sp^3$ -bonded materials that exhibit a wide range of ordered  
95 (repetitive) polytypes and disordered structures. It is proposed that *h-c*  $sp^3$ -bonded layered  
96 structures are also present in natural and laboratory-shocked diamonds, and these could account for  
97 the appearance of hexagonal features in the diffraction patterns<sup>10,11</sup>. The method of DIFFaX  
98 analysis, which had been used to interpret the diffraction patterns of layered stacking motifs in H<sub>2</sub>O  
99 ice, was applied to a range of impact diamonds and laboratory shocked samples to measure their  
100 degrees of 'hexagonality'- the percentage of hexagonal stacking units present in the structure<sup>10</sup>.  
101 This analysis approach supplemented by Monte Carlo techniques (MCDIFFaX) leads to the  
102 practical "stackogram" tool that was developed to identify and describe degrees of *h-c* ordered  
103 *versus* disordered layering patterns within the  $sp^3$ -bonded structures, and also to differentiate among  
104 samples that had experienced different shock regimes<sup>11</sup>. The possibility to engineer nanoscale

105 twinning among cubic and *h-c* diamond polytype structures adds additional capability to improving  
106 mechanical performance and thermal resistance<sup>17</sup>.

107

### 108 **sp<sup>2</sup>-bonded domains included within cubic-hexagonal sp<sup>3</sup>-bonded diamond structures**

109 Further to layered stacking disorder in diamond, additional structural complexity emerges when sp<sup>2</sup>-  
110 bonded carbon is brought into play. HRTEM studies of natural impact diamonds and laboratory-  
111 shocked materials have led to the recognition of sp<sup>2</sup>-bonded graphitic/graphene layered sequences  
112 occurring within the cubic/hexagonal diamond structures. These layered sequences are intimately  
113 associated with and coherently connected to the sp<sup>3</sup>-bonded domains, and the insertions of sp<sup>2</sup>-  
114 bonded regions are not repetitive<sup>13,14</sup>. A family of these nanostructural motifs could be related to  
115 the "diaphite" structures originally described to form at graphene surfaces following laser  
116 irradiation<sup>24</sup>. A series of density functional theory (DFT) calculations were undertaken to study the  
117 incorporation of graphitic/graphene-like sp<sup>2</sup> layers within the sp<sup>3</sup>-bonded domains<sup>14</sup>. The  
118 calculations revealed the possibility of entire families of mixed sp<sup>3</sup>-sp<sup>2</sup> bonded "diaphite"  
119 nanostructures existing within the energy-volume (E-V) phase space between graphitic and  
120 diamond-like polymorphs (Fig. 2). By comparison with the E(V) slopes corresponding to different  
121 compression regimes, the calculations gave insights into how these sp<sup>3</sup>-sp<sup>2</sup> bonded nanostructures  
122 might form within diamond-related materials as a result of static or shock-recovery HPHT treatment  
123 of diamond or graphitic precursors<sup>14</sup>. It is predicted that these diaphite structures can be produced  
124 either during the initial compression or within the rarefaction wave immediately following the  
125 initial shock impulse, followed by recovery to ambient conditions. These structures might also be  
126 formed metastably during ambient pressure synthesis using suitably designed precursors that can  
127 direct the layer-by-layer growth of nanostructured elements containing sp<sup>3</sup>- and sp<sup>2</sup>-bonded carbon  
128 centres, such as those implicated in the formation of functionally-active covalent organic  
129 frameworks (COFs)<sup>25</sup>. Tuning the sp<sup>3</sup>-sp<sup>2</sup> bonded nanomaterials towards nano- to macroscale  
130 composite structures might provide new families of next-generation diamond-related materials<sup>14,26</sup>  
131 (Fig. 3).

132

### 133 **sp<sup>3</sup>-bonded domains contained within mainly sp<sup>2</sup>-bonded graphitic materials**

134 The diaphite nanostructures extend across the E-V metastable phase diagram reaching towards fully  
135 sp<sup>2</sup>-bonded graphite (Fig. 2). It is interesting to examine the possibility that diaphane units might be  
136 included within predominantly graphitic structures. Cliftonite was described as a form of crystalline  
137 graphitic carbon exhibiting unusual cuboidal morphology within the Canyon Diablo iron meteorite  
138<sup>27</sup>. It is thought to form at low pressure by decomposition of iron carbide. Although the structure of  
139 cliftonite is currently presumed to be based solely on sp<sup>2</sup>-bonded graphitic layers it might also  
140 contain some sp<sup>3</sup>-bonded elements related to the increased mechanical resistance shown by some  
141 samples that have been studied. These sp<sup>3</sup>-bonded elements would be produced as a result of the  
142 shock wave generated during the impact of the Canyon Diablo asteroid with the Earth. A range of  
143 amorphous "hard carbon" materials produced by pyrolysis of carbonaceous precursors including  
144 sugar and cellulose are being developed for use as Na-ion battery anodes<sup>28</sup>. The molecular to  
145 nanoscale structure of these hard carbons is still under investigation but they are thought to consist  
146 of graphitic domains connected by fullerene-like structural units linked by some proportion of sp<sup>3</sup>-  
147 bonded carbon atoms<sup>28</sup>. Amorphous "diamond-like carbon" (DLC) materials prepared by vapour  
148 deposition methods contain a large proportion of sp<sup>3</sup>-bonded atoms within their structure and can  
149 achieve hardness values that rival those of crystalline diamond<sup>29</sup>. Other high-hardness carbons with  
150 mixed sp<sup>2</sup>-sp<sup>3</sup> bonding are derived from C<sub>60</sub> or C<sub>70</sub> fullerenes treated under HPHT conditions<sup>3</sup>.

151

### 152 **Towards further complexity among diamond nanostructures**

153 Rounded nanostructures exhibiting concentric layered geometry have been observed within  
154 partly graphitized diamonds and nanodiamonds and have been identified as "onion-like" or "bucky-  
155 diamond" structures<sup>16</sup>. Nanoparticles with these structures are thought to evolve by growth from  
156 central diamond cores as they transform into surrounding graphitic layers<sup>30</sup>. It is interesting to note

157 that the cubic diamond structure can achieve five and twelve-fold rotational symmetry through  
158 multiple twinning and could also engage in radially symmetric Mackay packing, especially among  
159 nanodiamonds such as those produced by detonation shock synthesis<sup>31,32</sup>. DFT studies of diaphite  
160 nanocomposite structures subjected to tensile stress conditions show a progressive transformation  
161 towards the graphitic phase, growing outwards from the sp<sup>2</sup>-sp<sup>3</sup> boundary<sup>26</sup>. This phenomenon that  
162 could be described as the "Mozzarella" solution resembles the surface graphitisation predicted for  
163 diamond under thermal stress<sup>33</sup>. This transformation mechanism certainly operates within natural  
164 and laboratory-shocked samples as they experience the rarefaction regime immediately following  
165 initial shock compression, and it could be generated within materials designed for applications that  
166 require linear or curved diamond-graphite interface structures.

167

### 168 **Prospects of engineering complex nanostructures within diamond-related materials**

169 To date, most of these fascinating and complex nanostructures have been identified among  
170 meteorite samples or impacted rocks, or in laboratory-shocked materials. The stacking-disordered  
171 and nanotwinned sp<sup>3</sup>-bonded materials can be described as diamond-related structures to be  
172 considered alongside the ordered cubic and hexagonal diamond polytypes. Stacking-disordered  
173 diamond structures are found to be prevalent among millimetre-sized samples obtained using large  
174 volume hydraulic press apparatus<sup>10</sup>. The sp<sup>2</sup>-bonded layers observed by HRTEM within shocked  
175 diamond presumably constitute a small fraction of the overall volume and can be considered as non-  
176 periodically inserted graphene regions within the sp<sup>3</sup>-bonded matrix. In this case, they do not yet  
177 constitute new diamond-related phases. However, DFT calculations demonstrate the stability of  
178 periodically extended and structurally coherent diaphite nanostructures with different relative  
179 thicknesses of the sp<sup>2</sup>- and sp<sup>3</sup>-bonded units<sup>14</sup>, indicating that such nanostructured assemblies  
180 might be engineered in bulk or thin film form by chemical or physical vapour (CVD, PLD) or  
181 atomic layer (ALD) deposition from atomic or molecular reactive gases. Diaphite nanostructures  
182 have already been produced in the laboratory by laser irradiation of graphene or graphite surfaces  
183<sup>25,34</sup> and similar features are suggested to appear at the diamond surface during thermal degradation  
184<sup>33</sup>. Other sp<sup>2</sup>-sp<sup>3</sup> bonded nanostructures could be achieved within diamond-related materials by  
185 designed shock-recovery conditions, while unusual carbon morphologies and nanostructured  
186 domains with unexpected symmetry properties are known to result from rapid diffusion and  
187 exsolution of C from metal carbide phases during the processing of steels<sup>34</sup>. It is certain that the  
188 formation and production of complex nanostructures within diamond-related nanomaterials is just  
189 entering its infancy. Advances in understanding these complex nanoscale architectures and  
190 developing targeted engineering approaches for technological applications will require  
191 comprehensive knowledge of the structural relationships and formation conditions of the sp<sup>2</sup>-sp<sup>3</sup>  
192 bonded nanostructures as well as transformation mechanisms between the two<sup>13,25,35,36</sup> (Fig. 3).

193

### 194 **References**

- 195 1. Hazen, R.M., Downs, R.T., Jones, A.P. & Kah, L. Carbon mineralogy and crystal chemistry. *Rev. Mineral.*  
196 *Geochem.* **75**, 7-46 (2013).
- 197 2. Linde, O., Geyler, O. & Epstein, A. The Global Diamond Industry [www.bain.com](http://www.bain.com) (2018).
- 198 3. Brazhkin, V. V. & Solozhenko, V. L. Myths about new ultrahard phases: Why materials that are significantly  
199 superior to diamond in elastic moduli and hardness are impossible. *J. Appl. Phys.* **125**, 130901 (2019).
- 200 4. Avery, P. et al. Predicting superhard materials via a machine learning informed evolutionary structure search.  
201 *npj Comput Mater.* **5**, 89 (2019).
- 202 5. Falcao, E.H.L. & Wudl, F. Carbon allotropes: beyond graphite and diamond. *J Chem Technol Biotechnol* **82**,  
203 524-531 (2007).
- 204 6. Geim, A.K. & Novoselov, K.S. The rise of graphene. *Nat. Mater.* **6**, 183-191 (2007).
- 205 7. Kaiser, K. et al. An sp-hybridized molecular carbon allotrope, cyclo [18] carbon. *Science* **365**, 1299-1301  
206 (2020).
- 207 8. Oganov, A.R., Hemley, R.J., Hazen, R.M. & Jones, A.P. Structure, bonding, and mineralogy of carbon at  
208 extreme conditions. *Rev. Mineral. Geochem.* **75**, 47-77 (2013).
- 209 9. Hoffmann, R., Kabanov, A. A., Golov, A. A. & Proserpio, D. M. Homo Citans and carbon allotropes: For an  
210 ethics of citation. *Angew. Chem. Int. Ed.* **55** **37**, 10962–10976 (2016).

- 211 10. Salzmann, C. G., Murray, B. J. & Shephard, J. J. Extent of stacking disorder in diamond. *Diam.Relat*  
212 *Mater.* **59**, 69–72 (2015).  
213 11. Murri, M. et al. Quantifying hexagonal stacking in diamond. *Sci. Rep.* **9**, 10334 (2019).  
214 12. Németh, P. et al. Lonsdaleite is faulted and twinned cubic diamond and does not exist as a discrete material.  
215 *Nat. Commun.* **5**, 1-5 (2014).  
216 13. Garvie, L.A.J., Németh, P. & Buseck, P.R. Transformation of graphite to diamond *via* a topotactic mechanism.  
217 *Am. Mineral.* **99**, 531-538 (2014).  
218 14. Németh, P. et al. Diamond-graphene nanocomposite structures. *Nano Lett.* **20**, 3611-3619.  
219 15. Németh, P., Garvie, L.A.J. & Buseck, P.R. Twinning of cubic diamond explains reported nanodiamond  
220 polymorphs. *Sci. Rep.* **5**, 18381 (2015).  
221 16. Németh, P. & Garvie, L.A.J. Extraterrestrial, shock-formed, cage-like nanostructured carbonaceous materials.  
222 *Am. Mineral.* **105**, 276-281 (2020).  
223 17. Huang, Q. et al. Nanotwinned diamond with unprecedented hardness and stability. *Nature* **510**, 250-253  
224 (2014).  
225 18. Baek, W. et al. Unique nanomechanical properties of diamond–lonsdaleite biphases: combined experimental  
226 and theoretical consideration of Popigai impact diamonds. *Nano Lett.* **19**, 1570-1576 (2019).  
227 19. Bundy, F. P. & Kasper, J. S. Hexagonal diamond - A new form of carbon. *J. Chem. Phys.* **46**, 3437-3446  
228 (1967).  
229 20. Hanneman, R.E., Strong, H.M. & Bundy, F.P. Hexagonal diamonds in meteorites: Implications. *Science* **155**,  
230 995-997 (1967).  
231 21. Frondel, C. & Marvin, U.B. Lonsdaleite, a hexagonal polymorph of diamond. *Nature* **217**, 587-589 (1967).  
232 22. Kraus, D. et al. Nanosecond formation of diamond and lonsdaleite by shock compression of graphite. *Nat.*  
233 *Commun.* **7**, 1-6 (2016).  
234 23. Turneure, S. J., Sharma, S. M., Volz, T. J., Winey, J. M. & Gupta, Y. M. Transformation of shock-  
235 compressed graphite to hexagonal diamond in nanoseconds. *Sci. Adv.* **3**, 3561 (2017).  
236 24. Ohnishi, H. & Nasu, K. Generation and growth of sp<sup>3</sup>-bonded domains by visible photon irradiation of  
237 graphite. *Phys.Rev. B* **80**, 014112 (2009).  
238 25. Shi, X. et al. Layer-by-layer synthesis of covalent organic frameworks on porous substrates for fast molecular  
239 separations. *ACS Appl Nano Mater* **1**, 6320-6326 (2018).  
240 26. Zhang, S. et al. Ultrastrong  $\pi$ -Bonded interface as ductile plastic flow channel in nanostructured diamond, *ACS*  
241 *Appl. Mater. Interfaces* **12**, 4135–4142 (2020)  
242 27. Brett, R. & Higgins, G.T. Cliftonite: A proposed origin, and its bearing on the origin of diamonds in  
243 meteorites. *Geochim. Cosmochim. Acta* **33**, 1473-1484 (1969).  
244 28. Dou, X. et al. Hard carbons for sodium-ion batteries: structure, analysis, sustainability, and electrochemistry.  
245 *Mater. Today* **23**, 87-104 (2019).  
246 29. Wei, Q. & Narayan, J. Superhard diamondlike carbon: preparation, theory, and properties. *Int Mater Rev* **45**,  
247 133-164 (2000).  
248 30. Xu, Q. & Zhao, X. Bucky-diamond versus onion-like carbon: End of graphitization. *Phys. Rev. B* **86**, 155417  
249 (2012).  
250 31. Shevchenko, V.Y. & Madison, A. E. Icosahedral diamond. *Glass Phys Chem* **32**, 118-121 (2006).  
251 32. Hofmeister, H. Fivefold Twinned Nanoparticles. *Encyclopedia of Nanoscience and Nanotechnology* Ed.  
252 Nalwa, H.S., Vol. 3, p. 431-452 (American Scientific Publishers, Stevenson Ranch, CA, 2004).  
253 33. De Vita, A. et al. A microscopic model for surface-induced diamond-to-graphite transitions. *Nature*, **379**, 523–  
254 526 (1996).  
255 34. Stefanescu, D.M., Alonso, G., Larrañaga, P., De la Fuente, E. & Suarez, R. A. comparative study of graphite  
256 growth in cast iron and in analogous systems. *Int J Metalcasting* **12**, 722-752 (2018).  
257 35. Yuan, Q., Lin, C.-T. & Chee, K.W.A. All-carbon devices based on sp<sup>2</sup>-on-sp<sup>3</sup> configuration. *Appl. Phys. Lett.*  
258 **7**, 020901 (2019).  
259 36. Xie, Y.-P., Zhang, X.-J., & Liu, Z.-P. Graphite to diamond: origin for kinetics selectivity. *Journal of the*  
260 *American Chemical Society* **139**, 2545–2548 (2017).  
261

## 262 Acknowledgements

263 PN acknowledges support from the Hungarian National Research, Development and Innovation  
264 Office project NKFIH\_KH126502, the János Bolyai Research Scholarship, and ÚNKP-19-4-PE-4  
265 New National Excellence Program of the Ministry for Innovation and Technology. LAJG. was  
266 supported by NASA Emerging Worlds grant NNX17AE56G. CGS received funding from the  
267 European Research Council under the European Union Horizon 2020 research and innovation  
268 programme (grant agreement No 725271). MM was supported by the IMPACT (R164WEJAHH)  
269 and the TRUE DEPTHS (ERC grant 714936) projects to Matteo Alvaro. MM also received support  
270 from the Barringer Family Fund for Meteorite Impact Research. We are grateful to the staff and for

271 use of the facilities in the John M. Cowley Center for High Resolution Electron Microscopy at  
272 Arizona State University. Our computational studies made use of the ARCHER UK National  
273 Supercomputing Service (<http://www.archer.ac.uk>) via the UK's HEC Materials Chemistry  
274 Consortium, which is funded by EPSRC (EP/ L000202). K.M. also acknowledges HPC resources  
275 provided by the UK Materials and Molecular Modelling Hub, partly funded by EPSRC  
276 (EP/P020194/1), and UCL Grace and Kathleen HPC Facilities and associated support services.

277

### 278 **Competing interests**

279 The authors declare no competing interests.

280

### 281 **Author list and affiliations**

282 Péter Németh<sup>1,2</sup>, Kit McColl<sup>3</sup>, Laurence A.J. Garvie<sup>4</sup>, Christoph G. Salzmann<sup>5</sup>, Mara Murri<sup>6</sup> and  
283 Paul F. McMillan<sup>5\*</sup>

284

285 <sup>1</sup>*Institute of Materials and Environmental Chemistry, Research Centre for Natural Sciences,*  
286 *Magyar tudósok körútja 2, 1117 Budapest, Hungary;* <sup>2</sup>*Department of Earth and Environmental*  
287 *Sciences, University of Pannonia, Egyetem út 10, H-8200, Veszprém, Hungary;* <sup>3</sup>*Department of*  
288 *Chemistry, University of Bath, Bath BA2 7AY, UK;* <sup>4</sup>*Center for Meteorite Studies, Arizona State*  
289 *University, Tempe, Arizona 85287-6004, USA;* <sup>5</sup>*Department of Chemistry, University College*  
290 *London, 20 Gordon Street, London WC1H 0AJ, UK;* <sup>6</sup>*Department of Earth and Environmental*  
291 *Sciences, University of Pavia, Via A. Ferrata, 1 27100 Pavia, Italy †*

292 \*e-mail: [p.f.mcmillan@ucl.ac.uk](mailto:p.f.mcmillan@ucl.ac.uk)

293

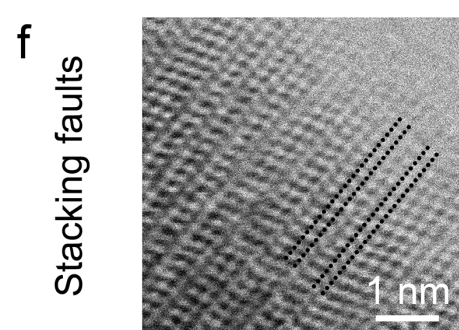
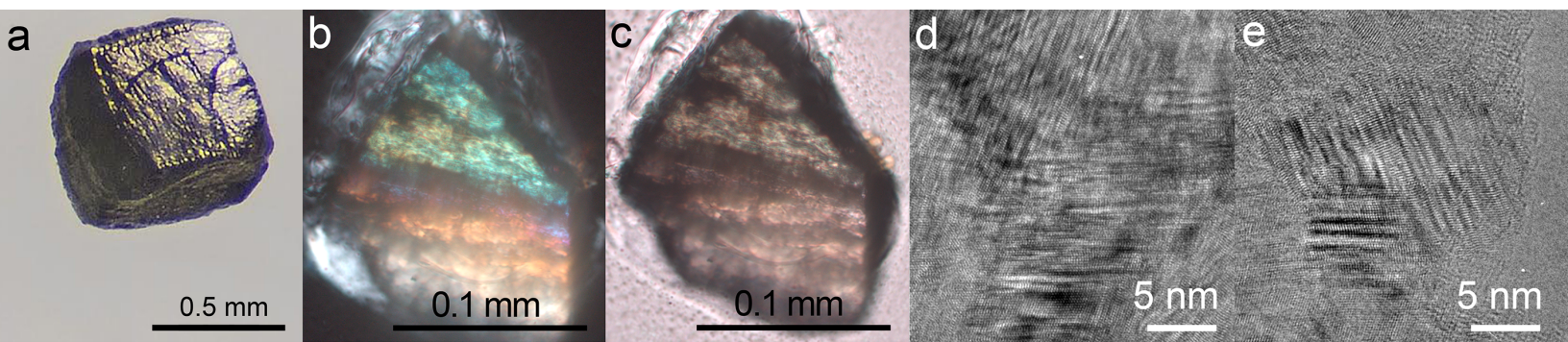
294 † *Now at: Department of Earth and Environmental Sciences, University of Milano-Bicocca, Piazza*  
295 *della Scienza 4, I-20126 Milano, Italy*

296 **Figure 1. Structural complexity in diamond.** **a**, A cubic diamond grain from Canyon Diablo meteorite<sup>12</sup>.  
297 **b,c**, optical micrographs from a fragment of a Popigai impact sample taken in normal (b) and polarized (c)  
298 light showing the presence of striations associated with regions of different birefringence at the micrometre-  
299 scale. **d,e**, Low magnification TEM images from fragments of the Canyon Diablo sample that reveal a range  
300 of complex structures at the nanoscale. **f-i** different nanostructural elements imaged at high (atomic)-  
301 resolution (left column) that are observed in different naturally impacted and laboratory-shocked samples,  
302 with corresponding schematics of atomic structures (right column). Cubic-hexagonal  $sp^3$ -bonded stacking  
303 faults (f) and complex patterns of new types of nanotwins (green dotted line)<sup>12</sup> (g) are demonstrated to occur  
304 within diamond-related materials and are proposed to lead to improved mechanical properties. Type 1 (h)  
305 and Type 2 (i) diaphite nanostructures<sup>13,14</sup> are identified using a combination of HRTEM and DFT  
306 techniques in natural and laboratory-shocked diamond specimens. These unique nanostructures could be  
307 engineered to improve fracture toughness among diamond materials. **j**, HRTEM evidence in the left panel  
308 for core-shell  $sp^2$ - $sp^3$  bonded nanostructures observed in shock-formed meteorite and naturally- or  
309 laboratory-shocked samples, with its schematic in the right panel. **k**, HRTEM images of nanostructures  
310 revealing five- and twelve-fold rotational symmetries formed by multiple twinning and radially symmetric  
311 Mackay packing<sup>15,16,32</sup> in the left column, with schematics in the right column. Panels adapted with  
312 permission from: a,f,g, ref.<sup>12</sup>, Springer Nature Ltd; h, ref.<sup>13</sup>, Mineralogical Society of America; i, ref.<sup>14</sup>,  
313 American Chemical Society; j, ref.<sup>16</sup>, Mineralogical Society of America; k, ref.<sup>15</sup>, Springer Nature Ltd.

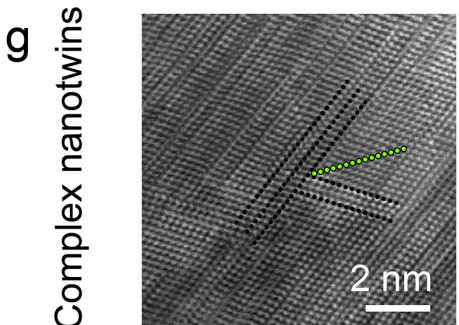
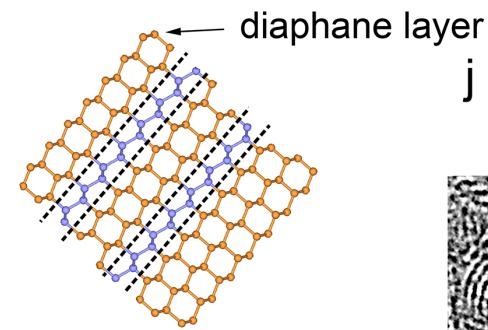
314  
315 **Figure 2. An energy-volume (E-V) map of crystalline carbon structures.** The relative E(V) relations for  
316 stable and metastable structures are established using density functional theory (DFT) calculations<sup>14</sup>. Known  
317 and predicted carbon allotropes from the SACADA database<sup>9</sup> are plotted as dark grey dots. The inset  
318 (rectangle) shows the range of energies for stacking disordered  $sp^3$ -bonded polytypes (turquoise) between  
319 cubic (3C) (orange dot) and the hexagonal (2H) diamond structure (blue)<sup>11</sup>. Points for Type 1 and Type 2  
320 diaphite structures described in<sup>14</sup> are shown as yellow and red dots, respectively. The two graphite points  
321 (green dots) correspond to the 2H and 3R polymorphs. Data for fullerene and single walled carbon nanotube  
322 crystalline structures are shown for comparison. The dashed line passing through the E(V) point for stable  
323 2H graphite constitutes a baseline for the datasets at T=0 K. Adapted with permission from ref.<sup>14</sup>, American  
324 Chemical Society.

325  
326 **Figure 3. Projected properties of diamond-related materials containing complex nanostructures.**  
327 **a**, Inclusion of cubic-hexagonal layer stacking polytype structures and nanotwinned domains within fully  
328  $sp^3$ -bonded diamond structures leads to increased bulk and shear moduli. Adding  $sp^2$  content in diaphite  
329 nanostructures maintains high elastic modulus values while contributing new features to the mechanical and  
330 other properties. Values for graphite, amorphous hard carbon and diamond-like carbon materials are  
331 indicated for comparison. **b**, Stress-strain relations under tension. Ideal diamond is predicted to achieve  
332 >40% longitudinal strain under application of tensile stresses up to ~220 GPa but real materials fracture at  
333 significantly lower stress-strain values due to defects within the  $sp^3$ -bonded structure. Graphene can be  
334 extended by over 25% before breaking. It is predicted that the presence of graphene-like domains within the  
335 diaphite structures should permit much greater lateral strain when subjected to lower tensile stresses  
336 depending on the width of the graphitic regions. **c**, The inclusion of diaphite nanostructures is expected to  
337 improve the fracture toughness of diamond materials as the energy of a propagating crack causes the  $sp^3$   
338 atoms at the graphene-diamond interface to transform into a graphitic state. **d**, Electronic properties.  
339 Inclusion of graphitic/graphene domains into diaphite nanostructures should result in the appearance of  
340 nanoconducting channels inside the insulating diamond matrix. **e**, Optical properties. The incorporation of  
341 graphitic regions into the diamond structure as well as internal scattering due to nanoscale domains and  
342 interface boundaries causes impact diamonds to appear black<sup>12</sup>. **f**, Thermal properties. The presence of  
343 layered polytype structures and nanoscale graphitic domains will hinder phonon propagation and cause the  
344 thermal conductivity to be significantly lowered compared with diamond or graphite (in plane). This can  
345 result in development of thermoelectric properties in diaphites containing nanoscale conducting channels.  
346 Panel e adapted with permission from ref.<sup>12</sup>, Springer Nature Ltd.

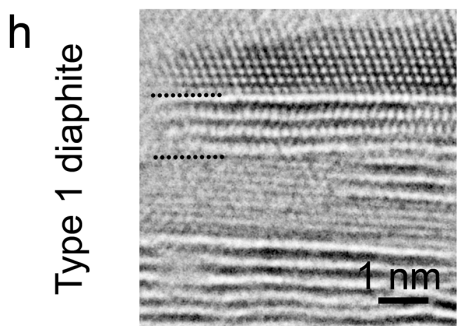
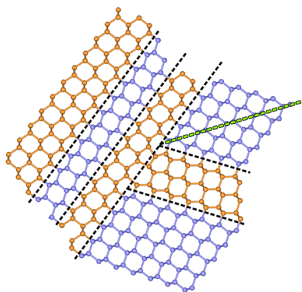
347  
348



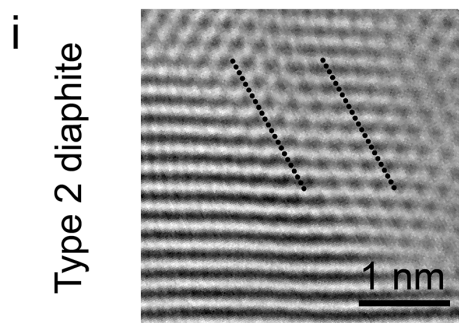
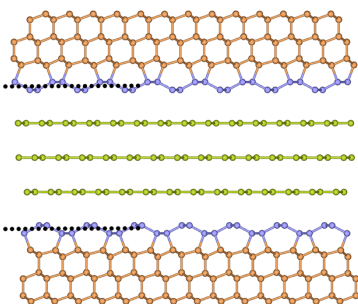
Stacking faults



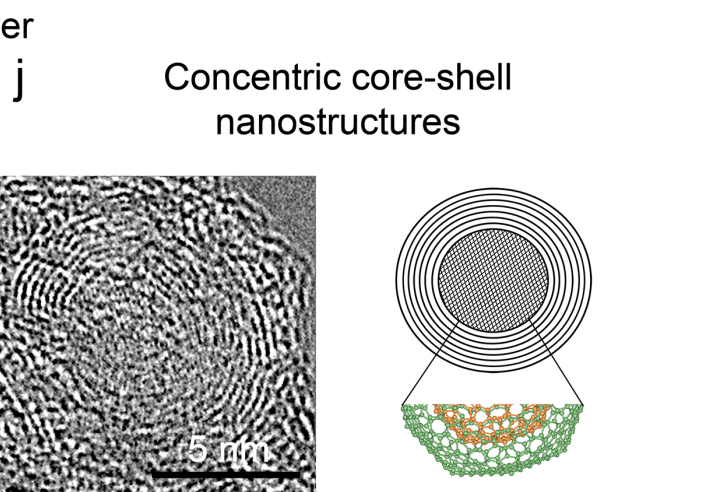
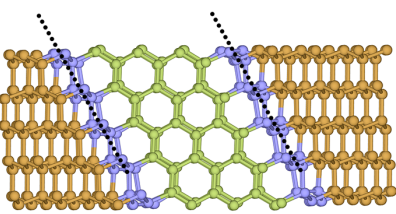
Complex nanotwins



Type 1 diaphite



Type 2 diaphite



**k** **Nanostructures with five- and twelve-fold rotational symmetry**

